


Thermoresponsive zwitterionic poly(phosphobetaine) microgels: Effect of macro-RAFT chain length and cross-linker molecular weight on their antifouling properties

Pabitra Saha^{1,2}  | Anand Raj Palanisamy^{1,3} | Marta Santi^{1,2} | Ritabrata Ganguly³ | Somashree Mondal^{1,4} | Nikhil K. Singha³ | Andrij Pich^{1,2,5}

¹DWI – Leibniz-Institute for Interactive Materials e.V., Aachen, Germany

²Institute of Technical and Macromolecular Chemistry, RWTH Aachen University, Aachen, Germany

³Rubber Technology Centre, Indian Institute of Technology Kharagpur, Kharagpur, India

⁴Department of Chemical Engineering, Indian Institute of Technology Guwahati, Guwahati, India

⁵Aachen Maastricht Institute for Biobased Materials (AMIBM), Maastricht University, Geleen, the Netherlands

Correspondence

Andrij Pich, DWI – Leibniz-Institute for Interactive Materials e.V., Aachen 52074, Germany
Email: pich@dwi.rwth-aachen.de

Funding information

Department of Science and Technology, Ministry of Science and Technology, Grant/Award Number: INT/FRG/DFG/P-04/2017; Deutsche Forschungsgemeinschaft, Grant/Award Numbers: 23535, PI 614/9-1

Abstract

Adsorption of proteins on biological surfaces is a detrimental phenomenon that reduces the work-life of the implants in various biomedical applications. Here, we synthesized a new class of thermoresponsive zwitterionic poly(phosphobetaine) (PMPC) microgel with excellent surface antifouling property by macro-RAFT mediated thiol-epoxy click reaction. End-group modified zwitterionic PMPC homopolymers with well-defined molecular weight and narrow dispersity were grafted onto poly(*N*-vinylcaprolactam-co-glycidyl methacrylate) (PVG) copolymer backbone followed by addition of a cross-linker, leading to microgel formation. While no upper critical solution temperature (UCST) was found in poly(*N*-vinylcaprolactam-co-glycidyl methacrylate-*g*-2-methacryloyloxyethyl phosphorylcholine) (PVGP) graft copolymers, the corresponding microgels exhibited both UCST and lower critical solution temperature (LCST) transitions, related to the swelling and collapse of PMPC and poly(*N*-vinylcaprolactam) (PVCL) components respectively. An increase in the molecular chain length of the PMPC increased the shifting of UCST and LCST of the microgels to higher temperatures, due to the ability of zwitterionic groups to coordinate a large number of water molecules. The effect of the variation in the molecular weights of amphiphilic poly(ethylene glycol) diamine (PEG-NH₂) cross-linker was also reflected in both temperature and salt responsiveness of the microgels. The efficacy of the microgels as potential antifouling materials was further studied by fluorescence microscopy and XPS analysis on microgel coatings treated with FITC-BSA solution and pure BSA solution respectively. Lower protein adsorption was observed for microgels grafted with higher molecular chain length of PMPC, whereas, the microgels synthesized using higher molecular weight PEG-NH₂ diamine cross-linker displayed greater protein adsorption on their surfaces.

KEYWORDS

antifouling, microgel, poly(phosphobetaine), RAFT, thermoresponsive

Pabitra Saha and Anand Raj Palanisamy contributed equally to this study.

This is an open access article under the terms of the Creative Commons Attribution License, which permits use, distribution and reproduction in any medium, provided the original work is properly cited.

© 2021 The Authors. *Polymers for Advanced Technologies* published by John Wiley & Sons Ltd.

1 | INTRODUCTION

Medical devices and implants require excellent resistance against the blood proteins to achieve their best performances under physiological conditions. Non-specific protein adsorption on surfaces, also called biofouling, is considered as the immune system's first response to implants. Several polymeric materials such as poly(ethylene glycol) (PEG)^{1,2} and poly(2-hydroxyethyl methacrylate) (PHEMA)^{3,4} have been known to prevent the protein adsorption. Nonetheless, the limitations in the use of oxidation-mediated degradation of PEG⁵ and relatively low water-solubility of high molecular weight PHEMA⁶ polymers prompted researchers to look for more efficient antifouling substitutes. Among the most promising alternatives to the abovementioned antifouling materials are zwitterionic polymers. Moreover, they have emerged as the "third-generation" antifouling materials because of their super hydrophilicity due to the formation of hydrogen bonds by stronger electrostatic interactions with the water molecules. The resemblance in their chemical structures to the biological membranes makes them biocompatible and superior to other antifouling materials.⁷

In recent years, there has been a plethora of reports on the synthesis of zwitterionic polymers with variable architectures.⁸ Swelling of polymer chains in the presence of salt solutions is a typical characteristic of polyelectrolyte materials, defined as the anti-polyelectrolyte effect,⁹ which enhances their ability to repel higher amounts of protein from biological substrates under physiological conditions. They are thermoresponsive as well because they exhibit a volume phase transition from a partially squeezed globule to a swollen coil state within a wide temperature window called upper critical solution temperature (UCST). Polyzwitterions, also known as polybetaines, are classified as sulfobetaine (SO_3^-), carboxybetaine (COO^-), phosphobetaine (PO_4^-) based on the type of anion present in the polymer backbone. For example, phosphobetaine methacrylate (MPC) type of monomer having anionic phosphate group and cationic quaternary ammonium group as the pendant group resembles the phospholipid layer phosphatidylcholine found in our cell membrane.¹⁰ Armes et al. reported the synthesis of poly(phosphobetaine) (PMPC) using atom transfer radical polymerization (ATRP) mechanism.¹¹ Surface-initiated ATRP (si-ATRP) technique have been proved to be a versatile approach for biomimetic PMPC monolayer formation ("grafting from" technique) and it was observed that there is a pronounced change in protein adsorption related to the variation of the chain length and density of PMPC- grafts. Although PMPC is a biocompatible material, the use of metal catalysts in ATRP processes leaves harmful residues on polymer surfaces, which limits their usage in biological applications. However, reversible addition fragmentation chain transfer (RAFT) helps in circumventing this limitation. PMPC synthesized in water via RAFT was first reported by Yusa et al. where they studied the micellization behavior of different copolymers and their application as anti-cancer drug carriers for pharmaceutical application.¹² Iwasaki et al. synthesized various block copolymers from PMPC-based macro-chain transfer agents (macro-CTA) with very low dispersity in all the cases.¹³ Until now, most studies related to PMPC polymers have been

conducted on bulk hydrogels and self-assembled monolayers (SAM).¹⁴ Utilizing the structural similarity of MPC to the phospholipid layer, Ishihara et al. used PMPC-grafted ultra-high molecular weight poly(ethylene) (UHMWPE) as an acetabular liner that reduces the wearing of the liner by increasing the lubrication due to hydration of biocompatible PMPC surface.¹⁵ Also, self-assembled monolayers (SAM) formed by polymers having non-fouling PMPC groups were effective in preventing adsorption of proteins.¹⁶⁻¹⁸

Although adequate studies have already explored this UCST-type transition based on poly(sulfobetaine) (PSB)¹⁹ and poly(carboxybetaine) (PCB) polymers of different architectures,²⁰ studies involving PMPC linear polymers and block copolymers have not reported both the UCST type transition and anti-polyelectrolyte behavior simultaneously. Kikuchi et al. synthesized high molecular weight PSB and PMPC linear polymers by si-ATRP mechanism and it was revealed that while PSB responds to the salt as external stimulus and leads to increase in size, PMPC remains almost unchanged.²¹ Therefore, the aim of this study is to produce thermoresponsive PMPC zwitterionic microgels with tunable UCST as well as anti-polyelectrolyte properties, which has not been explored in literature.

Stimuli-sensitive and colloiddally stable microgel particles are exploited in different fields of applications due to their high surface area and porosity.²² Different monomers have been used to fabricate microgels with different characteristics, which have made them suitable for different applications like drug delivery systems,²³ wastewater treatment,²⁴ oil recovery,²⁵ biosensors,²⁶ catalytic nano-reactors.²⁷ Among them, poly(*N*-isopropylacrylamide) (PNIPAM) and poly(*N*-Vinylcaprolactam) (PVCL) are the two most widely used materials because of their lower critical solution temperature (LCST) close to the physiological temperature ($\sim 32^\circ\text{C}$), where they switch from a swollen coil to collapsed globule state.²⁸ However, the synthesis of zwitterionic microgels has been proved to be challenging in the past few decades because of their high polarity and solvent selectivity.²⁹ Das et al. reported the synthesis of thermoresponsive PNIPAM microgels with sulfobetaine (SB) zwitterionic side groups via precipitation polymerization method and exploited the as-prepared P(SB-NIPAM) microgels as scaffolds for silver and gold nanoparticle synthesis.³⁰ Cheng et al. prepared carboxybetaine-based nanogels by inverse micro-emulsion polymerization, which showed improved long-term stability under the physiological conditions, by the virtue of low protein absorption ($\sim 0.3 \text{ ng/cm}^2$) in blood plasma.³¹ Andreas et al. reported the PNIPAM and PVCL-based zwitterionic microgels with sulfobetaine (SB) as the comonomer in the presence of sodium dodecyl sulfonate (SDS) surfactant. They observed a decrease in the particle size of the microgels and found that the molar incorporation of the sulfobetaine unit was about 30 mol%, explaining it as due to the co-surfactant behavior of the sulfobetaine units in aqueous solution.³² Previously, Schröder et al. synthesized microgels based on sulfobetaine with differently sized vinyl lactam rings in w/o inverse mini-emulsion polymerization.³³ Recently, we have reported PVCL-based zwitterionic sulfobetaine microgels via macro-RAFT approach in both precipitation polymerization and inverse mini-emulsion technique.^{34,35} Recently, Tian et al. have reported the synthesis of redox-responsive

bio-degradable zwitterionic PMPC nanogels with a diselenide type cross-linker via reflux precipitation polymerization and studied the drug release in the presence of different oxidant and reductants, which led to the degradation of the cross-linked network in the nanogels.²⁹

However, there are hardly any detailed reports on the systematic study of poly(phosphobetaine) (PMPC) microgels where their thermo-responsive behavior, anti-polyelectrolyte property, and protein-repelling characteristics are investigated simultaneously. Herein, we described the PMPC-PVCL microgel synthesis via macro-RAFT mediated thiol-epoxy click chemistry,³⁶ using an inverse mini-emulsion technique. The microgels were prepared by using PEG-based cross-linkers, which improved the swelling as well as the antifouling properties of the microgels. The variation in the molecular weight of the PMPC segment and PEG-NH₂ cross-linker was also found to be a key factor in the tuning of the aforementioned properties of the microgels. These microgels have potential to be used as antibio-adhesion coating and in temperature-triggered drug delivery applications as well.

2 | EXPERIMENTS

2.1 | Materials

Monomer, 2-methacryloyloxyethyl phosphorylcholine (MPC, molecular weight [MW] 295.27 g/mol, 97%), was purchased from Tokyo chemical industry (TCI) and used as received. *N*-vinylcaprolactam (VCL, MW 139.42 g/mol, 98%) and glycidyl methacrylate (GMA, MW 142.15 g/mol) were obtained from Sigma Aldrich and recrystallized and distilled before use. The thermal initiators 4,4'-azobis (4-cyanovaleric acid) (ABCVA, MW 280.28 g/mol, 98%), 2,2'-azobis (2-methylpropionitrile), (AIBN, MW 164.21 g/mol, 98%), the RAFT agent 4-cyano-4-(phenylcarbonothioylthio) pentanoic acid (CPCPA, MW 279.38 g/mol, 100%) and sodium borohydride (NaBH₄, MW 37.83 g/mol, 98%), and the cross-linkers poly(ethylene glycol) diamine (PEG-NH₂) of different molecular weights ($M_n = 3000, 6000, 10,000$ g/mol, 99.5%), and the solvents anisole, acetone, diethyl ether were purchased from Sigma Aldrich and used as received. The RAFT agent methyl 2-(ethoxycarbonothioylthio) propanoate (MECP, MW 208.29 g/mol) was synthesized as reported by Peng et al.³⁷ The regenerated cellulose membranes of different molecular weight cut-off (MWCO) were purchased from Carl Roth and washed with deionized water before use. Deionized water was used throughout all the reactions.

2.2 | Synthesis of poly(*N*-vinylcaprolactam-co-glycidylmethacrylate) (PVGn) random copolymer

The random copolymer of PVCL-co-PGMA (PVGn) (where, $n = 5$ mol % GMA) was synthesized by RAFT polymerization having a target molecular weight (M_n) of 5000 g/mol.³⁷ In a typical reaction, 1.000 g

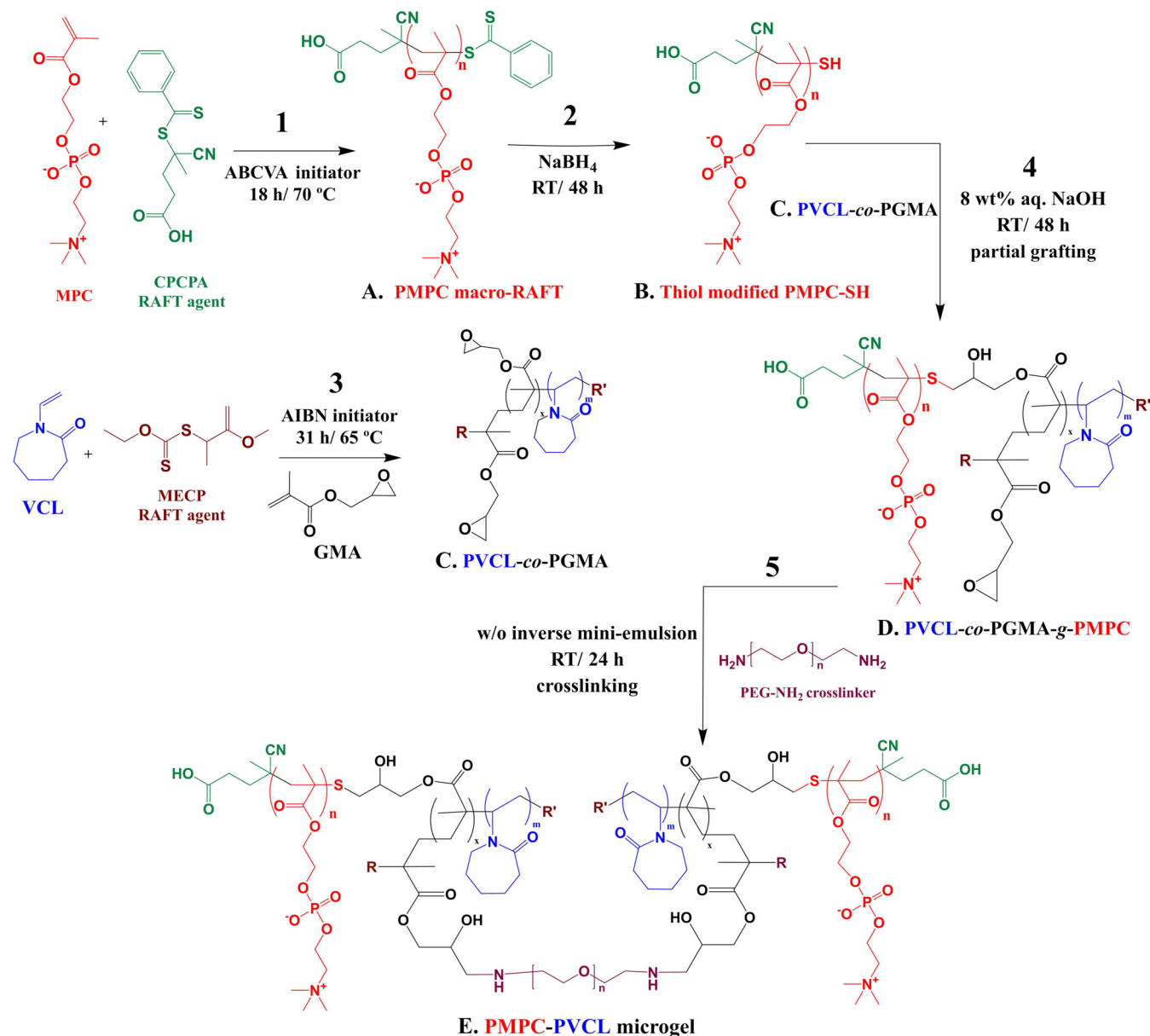
of VCL (7.170 mmol), 0.220 g of the RAFT agent MECP (the synthesis of MECP can be found in the supporting information, see Scheme S1) (1.050 mmol), and 0.006 g of the initiator AIBN (0.036 mmol) were taken in a 25 mL round bottom flask and purged with argon for about 30 min to remove oxygen from the system. In a separate ampoule, 0.054 g of GMA (0.371 mmol) with anisole were purged with argon. The reaction solution in round bottom flask was then heated to 65°C with continuous stirring and GMA was added through a syringe pump over 7 h. After 31 h, the reaction was stopped, exposed to the ambient atmosphere and rapidly cooled in ice bath and the product was precipitated from ice-cold diethyl ether. The obtained polymer was washed several times with the same solvent and dried under reduced pressure at 40°C overnight. After drying, the polymer was dissolved in water and dialyzed with a regenerated cellulose membrane of MWCO 3.5 kDa (Carl Roth, Germany) against water for 3 d. After freeze-drying, the white powder of PVCL-co-PGMA copolymer was obtained (yield ~60%, see Scheme 1. 3C).

2.3 | Synthesis of poly(2-methacryloyloxyethyl phosphorylcholine) homopolymer (PMPC macro-RAFT)

In a typical synthesis of PMPC 10000 macro-RAFT, 0.500 g of MPC monomer (1.693 mmol), 0.013 g of RAFT agent CPCPA (0.049 mmol), and 0.004 g of ABCVA initiator (0.016 mmol) were taken in a round bottom flask and dissolved in water/acetone (75/25, v/v) mixed solvents. The whole reaction mixture was then purged with argon for 30 min, following which the flask was kept in a pre-heated oil bath at 70°C for 18 h. After that, the resulting solution was precipitated from a large amount of acetone in an ice bath. The obtained polymer was then vacuum dried at 50°C overnight and re-dissolved in water followed by dialysis using regenerated cellulose membrane of MWCO 3.5 kDa for 4 days to remove unreacted monomer and RAFT reagent. Finally, the pure PMPC macro-RAFT was obtained as a light pinkish powder after freeze-drying (yield ~70%, see Scheme 1. 3A). (See NMR Figure 2B: ¹H NMR [in D₂O]: δ [ppm] = 4.1–4.4 (–OCH₂CH₂PO₄[–]CH₂), 3.6 (CH₂-N(CH₃)₂⁺, 3.2 (CH₂-N(CH₃)₂⁺).

2.4 | End group removal of PMPC macro-RAFT

The end group modification of the PMPC macro-RAFT was performed according to the procedure of Lowe et al.³⁸ In a typical end group removal of PMPC 10000, an aqueous solution of NaBH₄ (0.010 g, 25 equiv) was added to a PMPC macro-RAFT (0.200 g, 0.010 mmol) solution in water under an argon atmosphere and stirred for 48 h at room temperature (RT) to ensure the complete cleavage of the RAFT end group. The solution was dialyzed using a regenerated cellulose membrane with MWCO 3.5 kDa for 4 days. Thereafter, the solution was freeze-dried and obtained as an off-white powder, PMPC-10000 SH (yield ~80%, see Scheme 1. 3B).



SCHEME 1 Synthesis outline of zwitterionic microgel: 1. Synthesis of PMPC macro-RAFT, 2. end group removal of PMPC macro-RAFT, 3. synthesis of PVCL-co-PGMA random copolymer, 4. synthesis of PVCL-co-PGMA-g-PMPC graft copolymer, and 5. synthesis of PMPC-PVCL microgel

2.5 | Synthesis of PVCL-co-PGMA-g-PMPC (PVGPx)_y graft copolymer

The end-group-cleaved PMPC macro-RAFTs (PMPC-SH) with different molecular weights were partially grafted onto PVCL-co-PGMA random copolymer backbone in a thiol-epoxy click reaction. For the synthesis of (PVGPx)_y (where x = 7 is the mol% and y = 10,000 g/mol is the molecular weight of PMPC-SH), previously synthesized PVG5 (0.062 g, 0.014 mmol and GMA content 14 mol%) random copolymer dissolved in a mixture of water/acetone was added to an 8 wt% aqueous NaOH solution of PMPC-SH (0.080 g, 0.004 mmol) and stirred at RT for 24 h. The resulting solution was then dialyzed using a membrane of MWCO 12–14 kDa for 4 days to obtain the graft copolymer,

(PVGP7)₁₀₀₀₀ and finally freeze-dried to obtain a white powder (yield ~60%, see Scheme 1. 4D).

2.6 | Synthesis of PMPC-PVCL microgels

In the final step, the graft copolymers (PVGPx)_y with different molecular weights of PMPC-SH were crosslinked with poly(ethylene glycol) diamine (PEG-NH₂) cross-linker having different molecular weights to synthesize the PMPC-PVCL microgels. In a typical synthesis of MG-mKnX, (where m = 10 denotes 10,000 g/mol molecular weight of PMPC-SH and n = 3 denotes 3000 g/mol molecular weight of PEG-NH₂ cross-linker, X), 0.050 g of (PVG7)₁₀₀₀₀ graft copolymer and

0.015 g, 3 wt% of PEG-NH₂ (MW 3000 g/mol) cross-linker were dissolved in 1 mL of water (aqueous phase). The aqueous solution of the graft copolymer and cross-linker was then added to a 10 mL solution of toluene (oil phase) containing 250 mg of surfactant, Span 80 and an inverse mini-emulsion was obtained by ultrasound treatment at an energy level of 40% for 5 min (0.5 sec on-off) in a W-250 D Branson Digital Sonifier by setting an ice bath under the flask to keep the emulsion cool. The emulsion was then transferred to a stirring plate to react for 24 h at RT. After that, the emulsion was broken by centrifugation at 11,000 rpm for 15 min at a Heraeus Multifuge X3R centrifuge by Thermo Scientific using 5 mL of ethanol at first cycle and then twice with 20 mL of toluene. The solid residue was dialyzed using a dialysis membrane of 12–14 kDa for 7 days against deionized water and finally, the solution was freeze-dried to obtain a dry white microgel powder (~yield 50%, see Scheme 1. 5E).

2.7 | Sample preparation for XPS

All samples were cut from an Ultra-flat SiO₂ wafer (typ < 100>, Ted Pella) with an area of 1 cm², sonicated in 5 mL of acetone for 15 min, dried under N₂ flow, and then sonicated again in 5 mL ethanol for another 15 min and dried. To activate the surface and make it more prone to functionalization, all wafers were treated for 300 s with air plasma with 0.2 mbar pressure. The PVCL-coated sample was prepared by spin-coating a 1.5 mg/mL microgel dispersion (2000 rpm, 800 rpm/s as initial acceleration, for 1 min). The MG-40K10X zwitterionic microgel sample was prepared by spin-coating with 50 µL of a 4 mg/mL solution of the microgel at 2000 rpm (800 rpm/s as initial acceleration) for 1 min.

Protein adsorption on the surface was achieved by dipping the wafers in well plates filled with 3 mL of a bovine serum albumin (BSA) solution (100 mg/L) in phosphate buffer saline (PBS Buffer) (pH 7.4) at room temperature and the well plates were kept on a rocking platform at 60 rpm. After 3 h, the wafers were taken out, rinsed with 1 mL of PBS Buffer (pH 7.4) to remove the loosely attached proteins, and dried in the air.

3 | ANALYTICAL METHODS

Nuclear magnetic resonance (NMR) spectroscopy. ¹H NMR spectra were recorded on a Bruker DPX400 FT liquid NMR spectrometer at 400 MHz with D₂O as a solvent unless otherwise stated in the description of the diagram. The NMR spectra were analyzed using the MestReNova (version 11.0) software. The sample concentration was maintained at 5 mg in 0.4 mL of solvent.

Gel permeation chromatography (GPC). To determine the molecular weights (M_n and M_w) of the synthesized PMPC homopolymers and (PVGn) copolymers, GPC studies were carried out in two different GPC systems. For PMPC, aqueous GPC data was taken on one precolumn (8 × 50 mm) and three Suprema-Lux columns (8 × 300 mm) by Polymer Standard Service using an Agilent 1200

high-performance liquid chromatography pump. The flow rate was 1.0 mL/min. The experimental temperature was kept 40°C for the PMPC macro-RAFT homopolymers and 25°C for the (PVGx)_y grafted samples. The diameter of the gel particles was measured 5 µm with a nominal pore width of 30, 1000, and 1000 Å. An aqueous phosphate buffer (0.02 M, pH 8) (HiPerSolv CHROMANORM HPLC grade, VWR) was used as eluent. Calibration was performed using narrowly distributed poly(ethylene glycol) (PEG) standards (Polymer Standards Service). For the determination of molecular weights of PVGn copolymer, dimethylformamide (DMF) containing lithium bromide (LiBr, 1 mg/mL) was used as an eluting agent at a flow rate of 1.0 mL/min. A high-pressure fluid chromatography siphon (Bischoff HPLC Compact siphon) and a refractive index locator (Jasco RI-2031 or more) were utilized. Three sections with PSS GRAM gel were applied: each column length 300 mm, diameter 8 mm, the gel particles diameter 5 mm, nominal pore widths 50, 100, 1000, and 10,000 Å. An adjustment was accomplished utilizing poly(methyl methacrylate) (PMMA). All the GPC data were analyzed using the WinGPC UniChrom program (version 8.3.2).

Fourier transformed infrared spectroscopy (FTIR). FTIR spectra were recorded using a Thermo Nicolet Nexus FTIR spectrometer. Smart Splitpea as Attenuation Total Reflection (ATR) mode was used with silicon (Si crystal) as a base with a spectral resolution of 4 cm⁻¹. To obtain a good signal to noise ratio, an average of more than 200 scans were performed for each spectrum. The data were then analyzed using the Origin Pro (version 9.1) software.

Ultraviolet-visible (UV-vis) spectrophotometry. UV-vis spectra were recorded in a Varian Carry 100 Bio UV-vis spectrophotometer. The measurements were run at room temperature for the PMPC macro-RAFT and PMPC-SH samples. The temperature controller was associated with a UV-vis spectrophotometer to determine the cloud points of the graft copolymer and microgel samples. The samples were prepared with a concentration of 5 mg/mL in all the cases and measured in a temperature range between 5 and 65°C at 1°C interval at a wavelength of 500 nm. The data were analyzed using the program OriginPro (version 9.1).

Dynamic light scattering (DLS) study. DLS studies were performed on an ALV/CGS-3 compact goniometer system with ALV/LSE-5004 light scattering electronics and a multiple tau digital correlator. The samples were prepared by further diluting a microgel solution with water and filtration through a ChromafilXtra PET-120/25 filter with a pore size of 1.2 µm to remove any particulate matter. All measurements were made at an angle of 90°, at an attenuation time of 90 s and each measurement was repeated three times to have an average value of hydrodynamic radius (R_h) of microgels.

Atomic force microscopy (AFM). The morphology of the microgels was monitored by atomic force microscopy. Images were recorded using a NanoScope V from Veeco Instruments with an NCH-50 POINTPROBE-Silicon SPM-Sensor from Nanoworld in tapping mode. The sensor exhibited a resonance frequency of 320 kHz and a force constant of 42 N/m. For analysis of the obtained images, the free software Gwyddion 2.28 was employed.

X-ray photoelectron spectroscopy (XPS). To test the protein repellency of the polyzwitterionic microgel, SiO₂ wafers were spin-coated with the microgel dispersion, and XPS measurements were conducted using an Ultra Axis spectrometer (Kratos Analytical, Manchester). Si2p, S2p, C1s, and N1s core level signals were recorded in each sample. The samples were irradiated with monoenergetic Al K_α1,1 radiation (1486.6 eV) and the spectra were taken at a power of 144 W (12 kW × 12 mA). The curve-fitting analyses were performed subtracting a Shirley-type background and then using a Gaussian function to fit the experimental spectra. All analyzed spectra were energy referenced to the C1s signal of aliphatic C–C carbons located at 285.0 eV of binding energy (BE). Atomic ratios were calculated from peak intensities by using Scofield's cross-section values; the statistic error in semiquantitative XPS analysis is about 5% of the estimated value.

4 | RESULTS AND DISCUSSION

4.1 | Characterization of poly(*N*-vinylcaprolactam-co-glycidylmethacrylate) (PVGn) random copolymer

The RAFT agent, MECP was observed to be effective for the controlled polymerization of PVGn random copolymer.^{37,39} Due to its higher

reactivity, GMA was added gradually to the reaction mixture containing VCL monomer over a period of time to ensure that the GMA and VCL repeat units are arranged in a truly random manner. PVGn random copolymers with different GMA contents were characterized using ¹H NMR spectroscopy. The disappearance of the vinylic protons coming from both VCL (δ 4.4 and 7.2 ppm) and GMA (δ 5.4–5.8 ppm) monomers in the ¹H NMR spectrum (in CDCl₃ solvent) of PVGn copolymer proves the successful conversion of monomers to copolymer (see supporting information, Figure S2 for ¹H NMR). Furthermore, the GPC molecular weights (*M*_{n,GPC}) of the different PVGn copolymers were found to be well consistent with theoretical molecular weight having narrow dispersity (*D* = 1.16–1.23), suggesting the RAFT copolymerization occurred in a controlled manner (see Figure 1D). However, FTIR study was done to investigate the exact loading of GMA in the PVGn copolymer using a standard calibration line with PVCL-PGMA mixtures having known mol% of GMA (see Figure 1A,B) with respect to the 1620 cm⁻¹ (from the PVCL repeat units). From Figure 1C, an increase in peak intensities at 1720 cm⁻¹ (carbonyl stretching) and 845 cm⁻¹ (oxirane ring contraction) from GMA repeat units were observed in PVGn copolymer, which indicates the increase in incorporated GMA content on the copolymer backbone. The exact amount of GMA incorporated was found to be 14 and 12 mol% in the case of PVG5 and PVG10 samples, respectively.

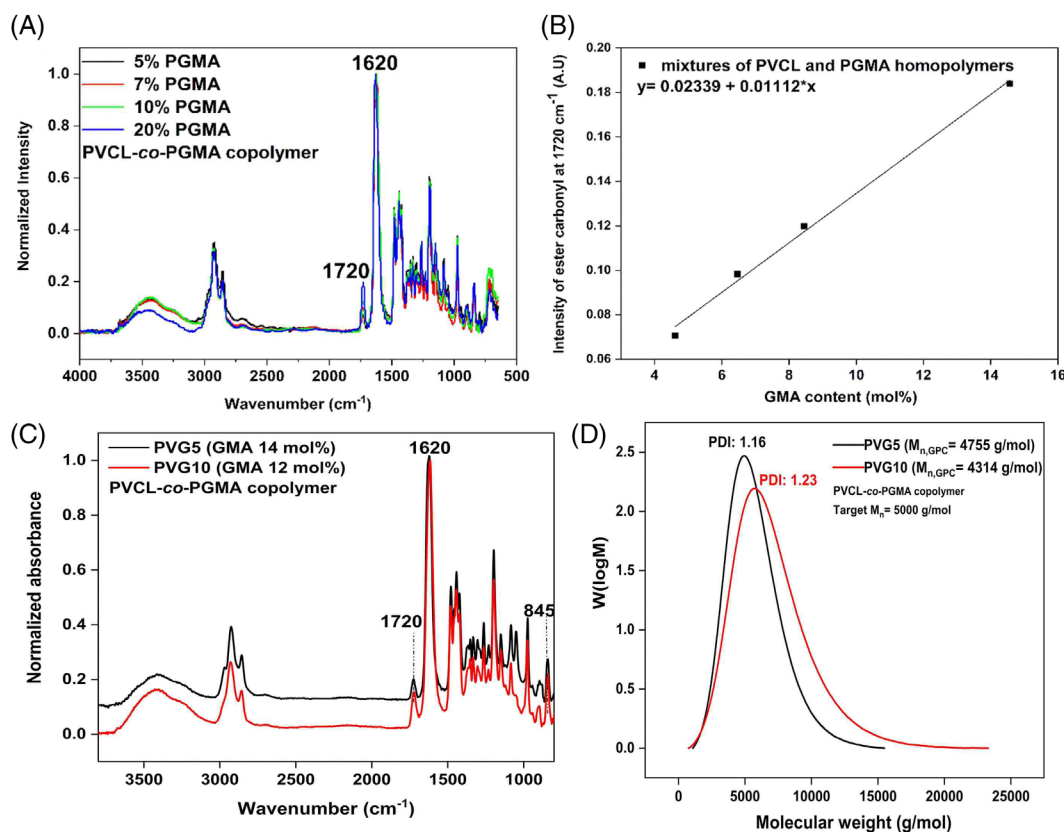


FIGURE 1 (A) FTIR spectra of a mixture of PVCL and PGMA linear homopolymers at a different known concentration of GMA (5, 7, 10, and 20 mol%) for calibration line construction, (B) calibration line drawn plotting the peak intensities of GMA at 1720 cm⁻¹ versus the known concentration of GMA, which follows the equation $y = 0.02339 + 0.01112x$ where, *x* is the GMA in mol%, (C) FTIR, and (D) GPC plot of PVG5 and PVG10 copolymers, respectively

4.2 | Characterization of PMPC macro-RAFT

The RAFT agent 4-Cyanopentanoic acid dithiobenzoate (CPCPA) was used in the polymerization reaction because it is compatible with most of the methacrylate monomers.¹² Four PMPC macro-RAFTs with different molecular weights (10,000, 20,000, 30,000, and 40,000 g/mol) were synthesized and characterized using ¹H NMR spectroscopy. Figure 2B shows that no vinylic proton (δ 5.4–5.8 ppm) from MPC monomer (Figure 2A) is left in the ¹H NMR of PMPC macro-RAFT and the appearance of aromatic protons (δ 7.5–8.0 ppm) suggests the successful incorporation of RAFT agent CPCPA at the tail-end of PMPC macro-RAFT. The NMR end-group analysis was carried out to calculate the molecular weight ($M_{n,NMR}$) of the zwitterionic PMPC macro-RAFTs, but $M_{n,NMR}$ was not definitive because increasing in target molecular weight of PMPC macro-RAFTs, the signal from the RAFT end-groups became weaker. However, aqueous GPC was done at 40 °C to determine the molecular weight ($M_{n,GPC-PMPC}$) of the PMPC macro-RAFTs (see Figure 3A), which concurred well with theoretical molecular weights ($M_{n,theo}$) (see Table 1) with low dispersity ($D_{PMPC} = 1.11$ –1.18) suggesting that CPCPA is an effective RAFT agent for the polymerization of zwitterionic methacrylate monomers.

FTIR studies were also performed and from Figure 3B, it can be found that the stretching vibrations of MPC monomer at 1638 cm⁻¹

due to its >C=C< unsaturation signal diminished in PMPC macro-RAFT. Moreover, the presence of the characteristic peak signals at 1720, 1230, and 1060 cm⁻¹ due to ester carbonyl (>C=O), -C-O stretching in -POCH₂ and -P-O stretching in -PO₄⁻, respectively,⁴⁰ in both MPC and PMPC macro-RAFT spectra supports that the zwitterionic segments remained unaffected during the polymerization.

4.3 | Characterization of end-group modified PMPC-SH

The PMPC macro-RAFTs were modified by NaBH₄ reduction to produce functional polymers with active thiol end-group. To show the complete removal of the phenyl group from the RAFT tail-end, they were primarily characterized by ¹H NMR studies. The disappearance of the phenyl group (δ 7.5–8.0 ppm) in the respective NMR spectrum of PMPC-SH suggests the successful cleavage of the RAFT end-group moiety (see Figure 2C). The RAFT end-group removal was further confirmed from UV-vis studies. The presence of phenyl group at the tail-end of PMPC macro-RAFT was shown by a strong absorption peak at 305 nm (π - π^* transition),³⁵ which disappeared upon cleavage of the RAFT end-group by NaBH₄ reduction (see Figure 3C). In some cases, unfavorable reaction conditions

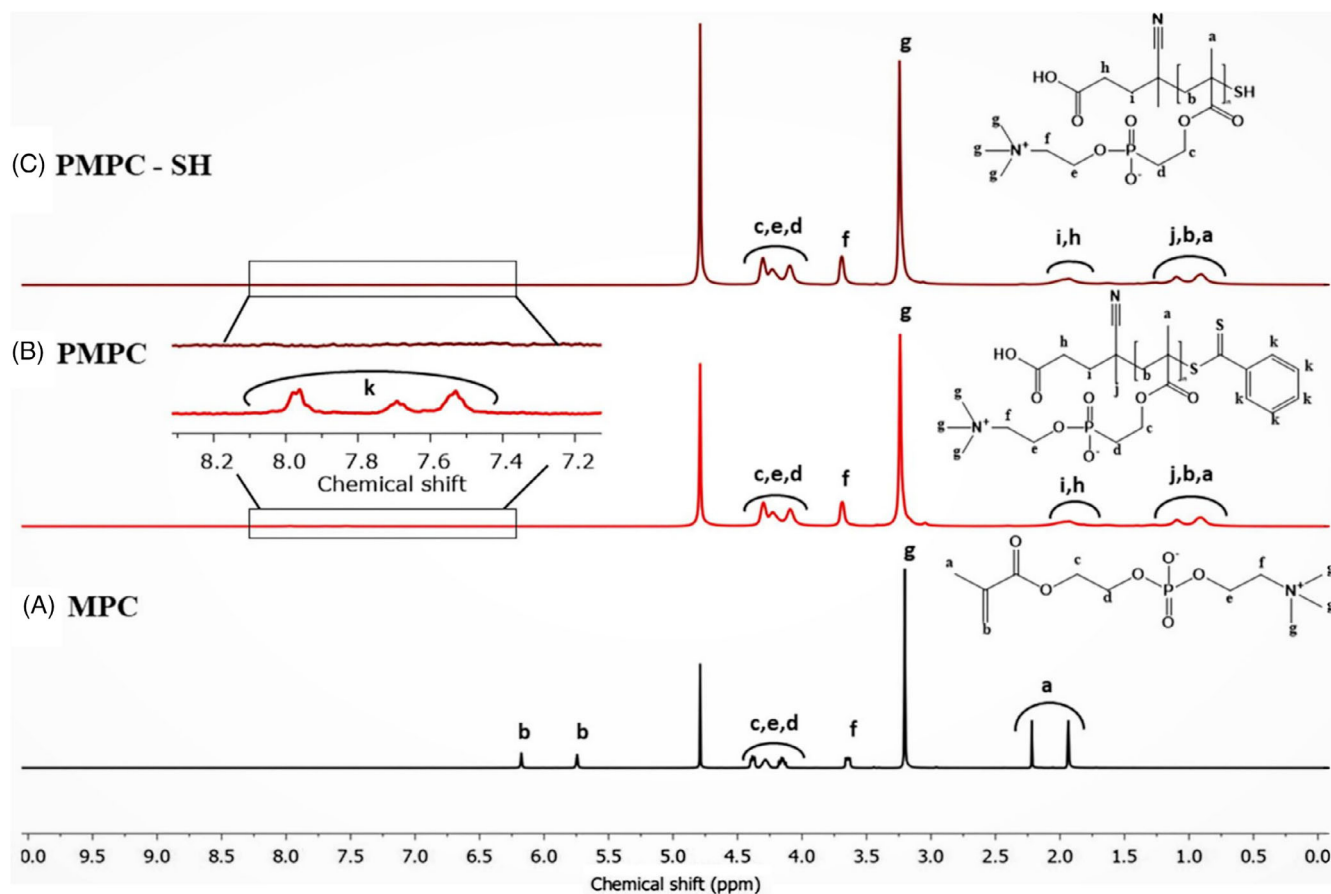


FIGURE 2 ¹H NMR spectral comparison between (A) MPC monomer, (B) PMPC 10000 macro-RAFT, and (C) end-group modified PMPC 10000-SH

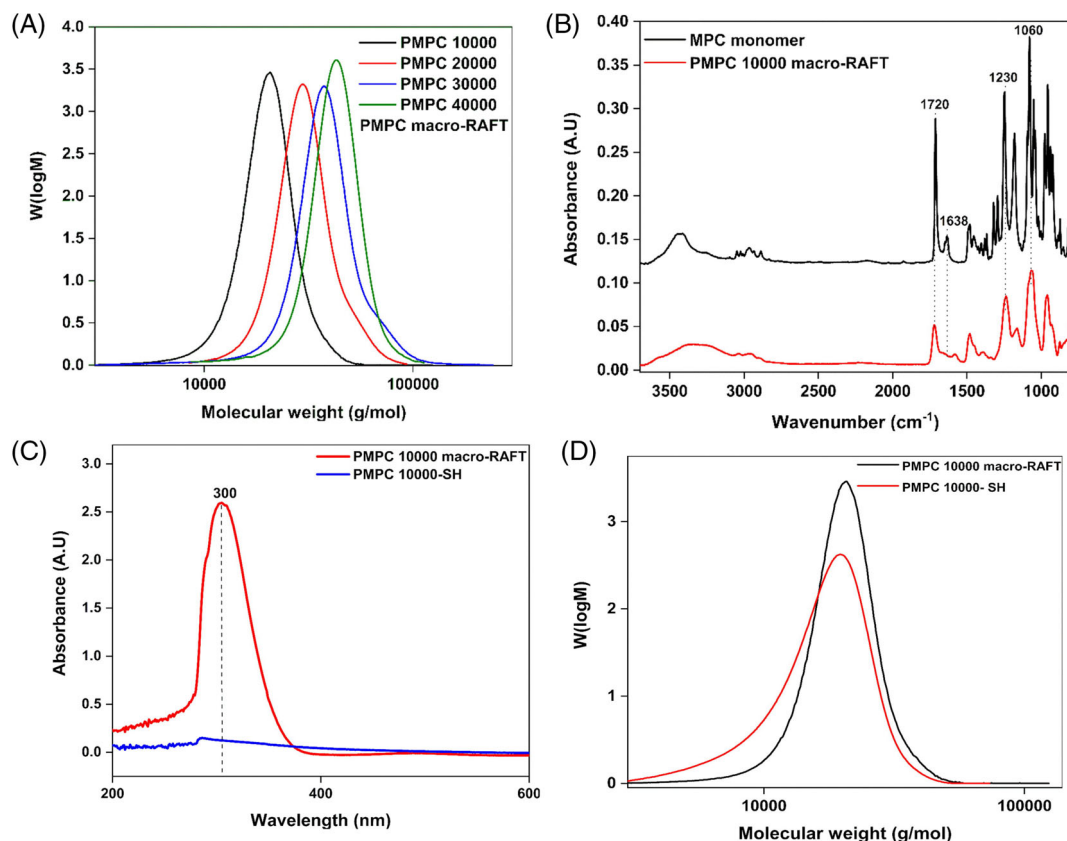


FIGURE 3 (A) GPC traces of different molecular weighed PMPC macro-RAFTs, (B) FTIR spectra of MPC monomer and PMPC 10000 macro-RAFT, (C) GPC traces, and (D) UV-vis spectra of PMPC macro-RAFT and PMPC 10000-SH end-group modified homopolymers, respectively

TABLE 1 Molecular weight and molecular weight distribution of different PMPC macro-RAFTs and end-group modified PMPC-SHs

PMPC macro-RAFT sample	Targeted molecular weight, $M_{n,theo}$ (g/mol)	Molecular weight obtained by NMR, $M_{n,NMR}$ (g/mol)	Molecular weight obtained by GPC, ${}^aM_{n,GPC-PMPC}$ (g/mol)	Dispersity (\bar{D}_{PMPC})	Modified PMPC homopolymers	Molecular weight obtained by GPC, ${}^aM_{n,GPC-SH}$ (g/mol)	Dispersity (\bar{D}_{SH})
PMPC 10000	10,000	22,700	18,600	1.11	PMPC-SH 10000	17,800	1.20
PMPC 20000	20,000	39,400	28,200	1.11	PMPC-SH 20000	27,800	1.19
PMPC 30000	30,000	62,500	34,800	1.18	PMPC-SH 30000	34,200	1.25
PMPC 40000	40,000	74,100	39,100	1.10	PMPC-SH 40000	39,400	1.23

^aAqueous GPC experiments were carried out using phosphate buffer (pH 8) at 40°C temperature.

may lead to the oxidative dimerization of thiol to disulfide (-S-S-) linkage³⁸ and might require extra steps to recover the thiol-ended polymer product, that is, using dithiothreitol (DTT) as a reducing agent. Often, this would result in impurities and lower yield of thiol end-group product. However, in this study, the RAFT end-group removal was done under an inert argon atmosphere, so that the modified PMPC-SH did not dimerize. This is proved from Figure 3D, where the modified PMPC-SH zwitterionic polymer did not show any hump in GPC traces and a very minimal change in the molecular weight ($M_{n,GPC-SH}$) was observed, suggesting the absence of any dimerized structures (see Table 1).

4.4 | Characterization of PVCL-co-PGMA-g-PMPC graft copolymer

The end-group modified PMPC-SH homopolymers were grafted onto PVGn random copolymer via partial substitution of GMA groups by thiol-epoxy click reaction. ¹H NMR studies validated the presence of characteristic proton signals deriving from PMPC-SH zwitterionic polymer and PVG copolymer (see Figure 4). The loading efficiency of zwitterionic polymer chains was calculated from the peak integral area of PMPC-SH (δ 3.78–3.57 ppm) and PVG (δ 2.70–2.22 ppm) and the exact incorporation of PMPC in graft copolymer was in good

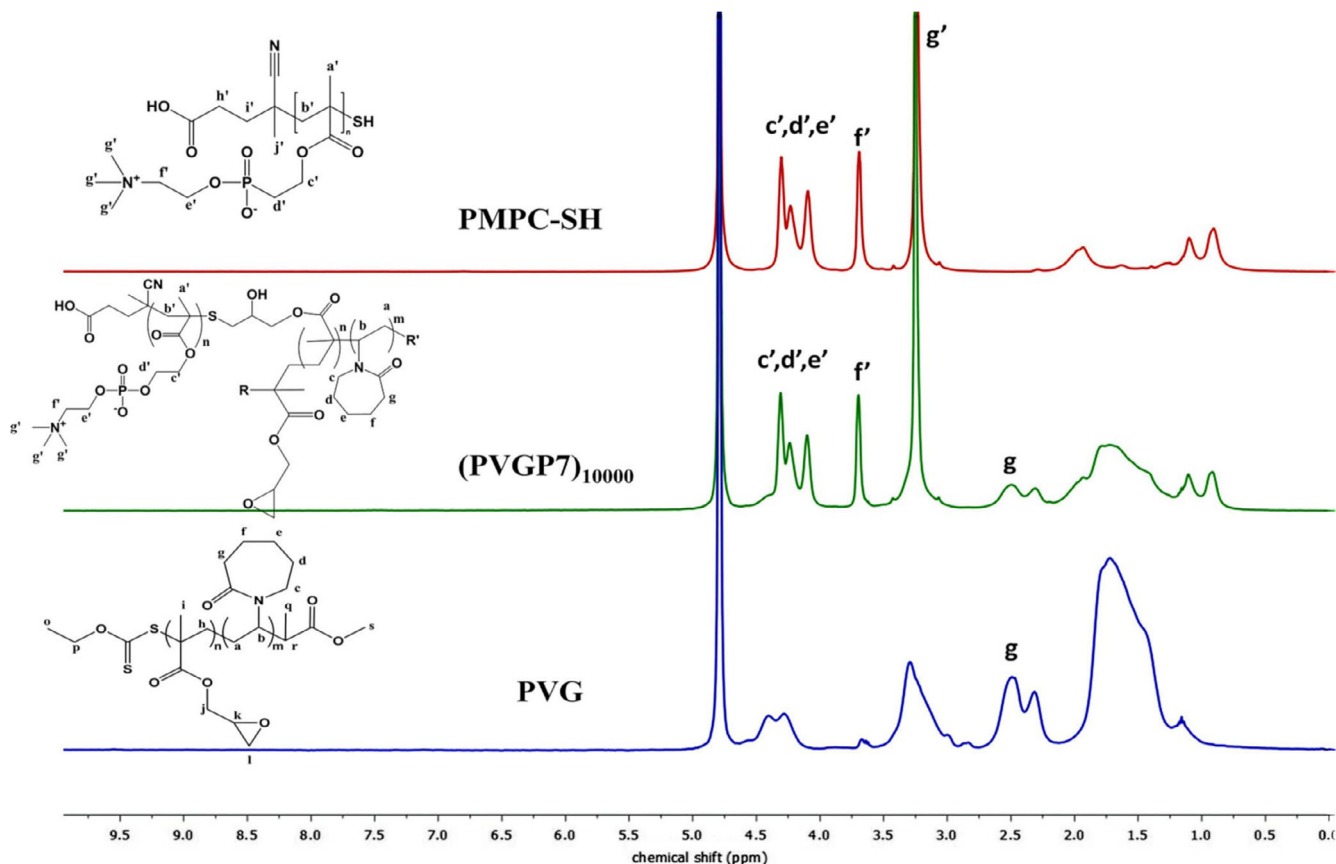


FIGURE 4 ^1H NMR spectra of (A) PVG copolymer, (B) PMPC-SH polymer, and (C) (PVGP7) $_{10000}$ graft copolymer

agreement with the feed molar amount having satisfactory conversion (see Table 2).

The successful “grafting to” approach in this particular synthesis of (PVGP $_x$) $_y$ graft copolymer was also confirmed by FTIR studies. Figure 5A illustrates the effective incorporation of PMPC-SH in the zwitterionic functional graft copolymer, displaying an increase in the intensity of 1720 cm^{-1} peak signal ($>\text{C}=\text{O}$ stretching) coming from both PGMA and PMPC-SH segments. Along with that, the significant decrease in characteristic peak intensity at 845 cm^{-1} of oxirane ring contraction strongly implies the insertion of the PMPC zwitterionic units to the PVG copolymer backbone by partial consumption of GMA groups via ring-opening (see inset of Figure 5A). Moreover, the higher the molecular weight of the PMPC-SH used, the higher is the intensity of the newly appeared characteristic peaks at 1230 and 1060 cm^{-1} due to the presence of $-\text{C}-\text{O}$ stretching in $-\text{POCH}_2$ and $-\text{P}-\text{O}$ stretching in $-\text{PO}_4^-$ functional groups, respectively, from the zwitterionic polymers as shown in Figure 5B.

Often in literature, it has been reported that the polymerization carried out via precipitation method incorporates lower amount of high molecular weight polyzwitterionic chains in thermo-responsive PVCL or PNIPAM microgels.³⁴ However in this study, an improvement in loading of higher molecular chain length polyzwitterions (PMPC) has been achieved using a “grafting to” technique.

The aqueous GPC analyses of different synthesized graft copolymers were performed at 25 °C (see Figure 5C), and results show that with the increase in molecular weight of PMPC, the corresponding graft copolymer samples eluted out of the GPC column at relatively shorter time along with a narrow molecular weight distribution, which suggests the successful grafting of higher molecular weight PMPC zwitterionic chains on the PVG copolymer backbone. However, a little shoulder in each of the GPC traces was observed due to the slightly higher dispersity (D_{graft}) index.⁴¹ Table 2 shows that the molecular weights of the graft copolymers obtained from GPC did not show good agreement with the targeted ones. This could be ascribed to the difference in the operating temperature of the GPC instrument. Due to the use of different temperatures, the hydrodynamic diameters of the PMPC homopolymer and graft copolymer at their respective coil states are different. In the case of (PVGP $_x$) $_y$ graft copolymer, 25 °C temperature was maintained to avoid the collapse of the PVCL chains that could have led to further discrepancies. Nonetheless, low molecular weight distributions (see Table 2) of graft copolymers suggest that the “grafting to” thiol-epoxy reaction occurred in a composed manner.

The strong influence of PMPC polyzwitterion incorporation on PVG copolymer (cloud point = 40 °C) was reflected in the cloud point analysis of (PVGP $_x$) $_y$ graft copolymer when a drastic shift in LCST-type phase transition was observed to higher temperatures (cloud

TABLE 2 The molar composition of (PVG P_x)_y graft copolymers with their cloud points

Graft copolymer sample	Molecular weight of PMPC-SH	Mol% of PMPC-SH (feed)	Mol% of PMPC-SH (exact)	Molecular weight of graft copolymer ^a ($M_{n,GPC-graft}$)	Molecular weight distribution (\mathcal{D}_{graft})	Cloud point (°C)
(PVG $P7$) ₁₀₀₀₀	10,000	7	3.0	8400	1.34	56
(PVG $P7$) ₂₀₀₀₀	20,000	7	3.5	14,600	1.22	58
(PVG $P7$) ₃₀₀₀₀	30,000	7	3.8	18,200	1.24	59
(PVG $P7$) ₄₀₀₀₀	40,000	7	4.2	20,200	1.28	60

^aAqueous GPC experiments were carried out using phosphate buffer (pH 8) at 25°C temperature.

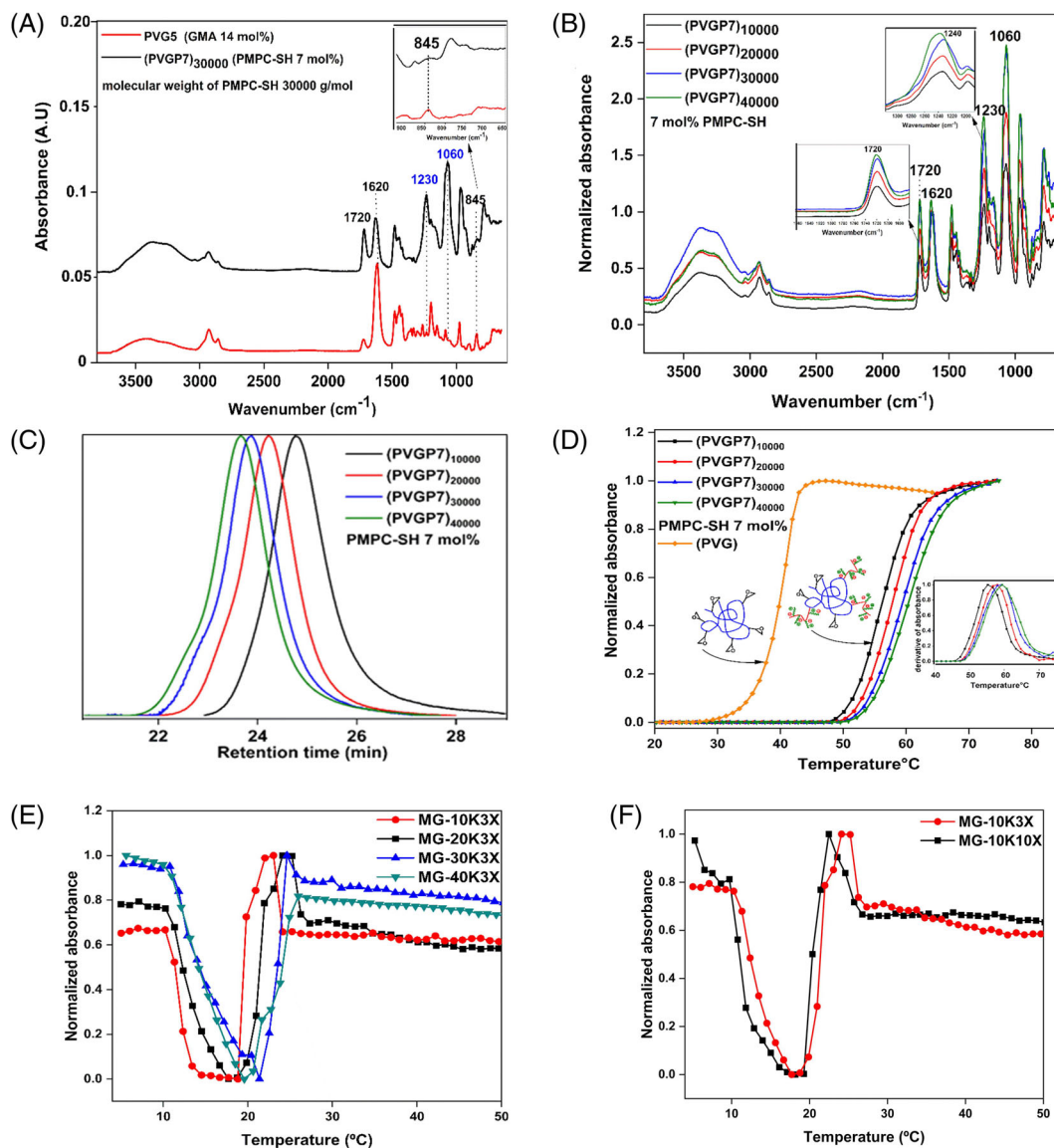


FIGURE 5 FTIR spectra spectral comparison between (A) PVG copolymer and (PVG $P7$)₃₀₀₀₀ (7 mol% PMPC-SH of 30,000 g/mol molecular weight), (B) different molecular weighed PMPC-SH incorporated graft copolymers, (C) GPC traces of different graft copolymers, and (D) cloud point of different graft copolymers, (E) Cloud point of microgels prepared with different molecular weight of PMPC, and (F) different molecular weight of cross-linkers (PMPC 10000), where 3X and 10X stand for PEG-NH₂ cross-linkers with 3000 and 10,000 g/mol molecular weights respectively

point = 56°C for (PVG $P7$)₁₀₀₀₀) in a temperature-controlled UV-vis spectrophotometric study (see Figure 5D). Due to the presence of

highly hydrophilic polar polyzwitterionic PMPC chains grafted on PVG copolymer backbone, the collapse of PVCL polymer chains demands

more thermal energy because PMPC chains form strong hydration layer with surrounding water molecules. Moreover, the higher the molecular weight of PMPC used, the higher was the cloud point of the respective graft copolymers, because of the increasing hydrophilicity of MPC zwitterionic repeat units. However, a proportionate shifting of cloud point with a progressive increase in PMPC molecular weight was not noticed when the derivative of cloud point absorbance was plotted (see inset of Figure 5D). This could be attributed to the unique hydrophobic hydration state of three methyl groups (attached to the quaternized N-atom) of PMPC with surrounding water molecules. Since the hydrophobic hydration became weaker with the higher molecular weight of PMPC, a considerable shift in the LCST with increasing PMPC molecular weight could not be observed.⁴²

4.5 | Characterization of PMPC-PVCL microgels

The microgels were synthesized via an amine-epoxy cross-linking reaction between the leftover GMA groups in (PVG_{Px})_y graft copolymer and amine groups in PEG-NH₂ cross-linkers.

The hydrodynamic radius trend in MG-3X series cross-linker (low molecular weight PEG-NH₂ 3000 g/mol) (see supporting information, Table S6) shows that the higher hydrophilic character of larger molecular weight PMPC led to the increase in hydrodynamic radius of the microgels. All of the microgels exhibit polydisperse size distribution as they were synthesized by a water-in-oil (w/o) mini-emulsion technique that was stabilized using large amount nonionic Span 80 surfactant and it was difficult to remove the impurities from the system even after subsequent centrifugation and dialysis steps (see supporting information, Table S6).

The dual thermoresponsive behavior was observed in all synthesized microgels when the temperature was varied from 5 to 50°C. They exhibited a prominent UCST-type transition below 20°C as the absorbance of the microgel solution decreased (appearance of transparency) due to the swelling of the PMPC chains. After a shorter temperature window, the crosslinked PVCL network collapsed and as a result, the absorbance of the microgel solution increased again (appearance of turbidity), termed as LCST-type transition. Interestingly, an increase in the PMPC molecular weight increased the UCST of the microgels as a higher number of zwitterionic repeating units in PMPC demanded higher thermal energies to form H-bonding with surrounding water molecules. Similarly, the LCST transition was also increased because swollen PMPC chains formed a strong hydration layer to resist the collapse of the crosslinked PVCL network easily (see Figure 5E).³⁵ The effect of the variation of the cross-linker molecular weight on thermoresponsive behavior was also noticed. Using higher molecular weight PEG-NH₂ cross-linker (10,000 g/mol), the synthesized microgels (MG-10K10X) showed a shifting of both UCST and LCST towards relatively lower temperatures as PMPC chains could only stretch out to a lower extent, because the PVG copolymer chains are held together in a more compact manner compared to the cross-linkers with lower molecular weight (3000 g/mol). Thus the

PVCL chains collapsed at lower temperatures to expel the entrapped water molecules (see Figure 5F).³⁵

Generally, polyelectrolytes are well known for their anti-polyelectrolyte behavior.⁴³ In the presence of different salt solutions, the coulombic force of attraction between the opposite charges in the zwitterionic backbone is overcome by the screening of salt-ions. As a result, the polyelectrolytic chains expand their arms by interacting with a large volume of water.⁴⁴ In our study, the zwitterionic PMPC-PVCL microgels responded to the various NaCl salt concentrations as well. The cross-linker molecular weight that strongly influenced the change in the size of PMPC-PVCL microgels also affected the salt responsiveness characteristics, showing a binary behavior of alternating polyelectrolyte and anti-polyelectrolyte at different salt concentrations.^{45,46} MG-10K3X microgel prepared with lower molecular weight (3000 g/mol) PEG-NH₂ cross-linker shows an increase in hydrodynamic radius initially up to 0.02 M NaCl salt concentration (anti-polyelectrolyte behavior), whereas higher molecular weight (10,000 g/mol) PEG-NH₂ cross-linker prepared microgel (MG-10K10X) shows the only reduction in microgel size even at the least concentration of NaCl (0.005 M) used. This is because the PMPC zwitterionic chains could not wriggle completely out of the crosslinked PVCL network, therefore, even 0.005 M concentrated NaCl solution affected the PVCL segments much directly interfering with the H-bonding between water and the polymer chains, exhibiting exclusively the polyelectrolyte-type behavior (see supporting information, Figure S7b).

5 | ANTIFOULING STUDY OF PMPC-PVCL MICROGELS

The antifouling property of the so-prepared zwitterionic PMPC-PVCL microgels was also investigated to experience the reduction in protein adsorption varying different parameters on a standard poly(ethersulfone) (PES) membranes (Pieper GmbH, Germany) with a pore size of 100 nm.

The fluorescein isothiocyanate-conjugated to bovine serum albumin (FITC-BSA) protein appears bright green under a fluorescence microscope at 25°C, so it was chosen as the standard protein solution for antifouling study. The FITC-BSA solution (100 mg/L) was applied to different microgel-coated surfaces to observe the change in color intensity. As expected, the blank membrane adsorbed most of the protein on its surface and appears intense green. The pure PVCL microgel-coated membrane shows almost the same color intensity as of the blank membrane as pure PVCL singularly does not have any protein-repelling properties. Interestingly, the membranes coated with zwitterionic PMPC-PVCL microgels show very light green (nearly dark) images due to their ability to repel away a large amount of protein from their surfaces efficiently, thereby proving themselves as a potential antifouling material (see Figure 6B). The leftover FITC-BSA protein solution was collected after treating the membranes and measured by a UV-vis spectrophotometer to find out the absorbance of the respective solutions because it was difficult to distinguish the difference in the color intensity of the fluorescence images of the membranes with the naked eye. The FITC-BSA protein shows a strong

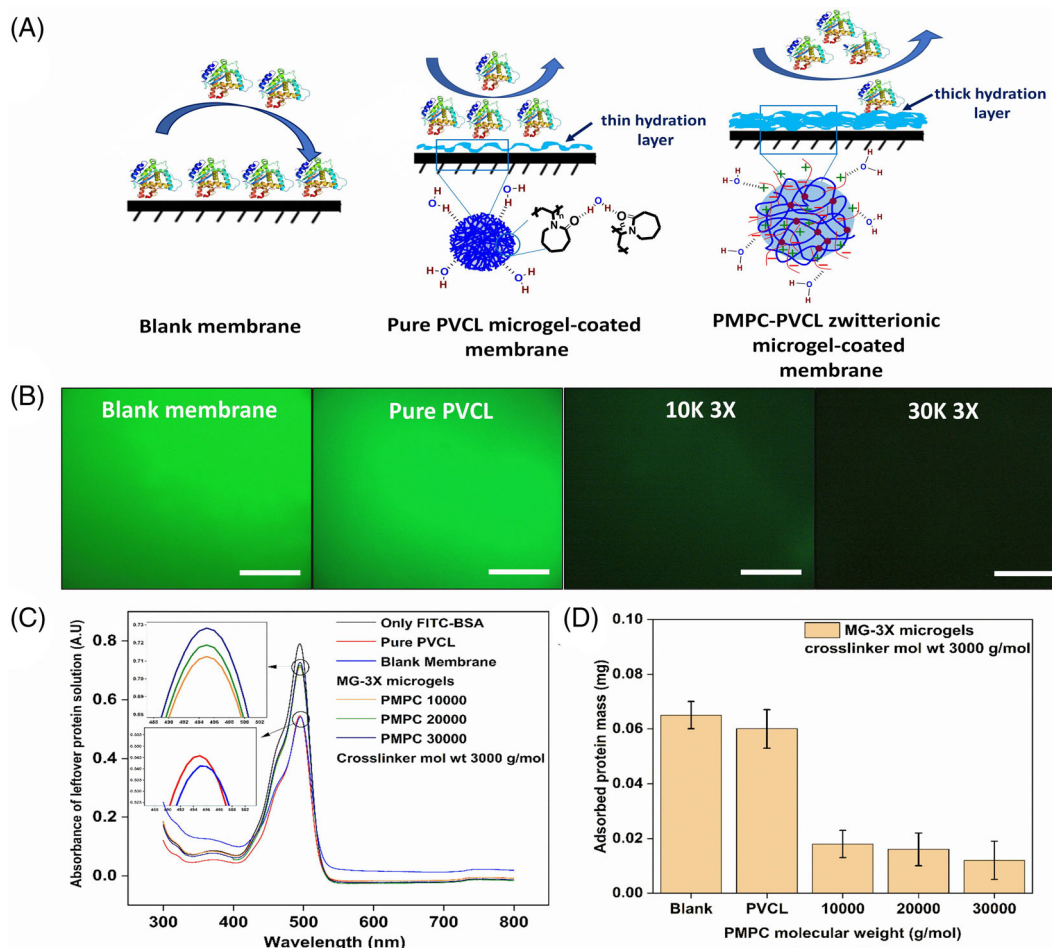


FIGURE 6 (A) Schematic representation of surface fouling using a different type of microgel coating (pure PVCL and PMPC-PVCL) (B) fluorescence microscopic images of different membranes after protein assay test; (from left to right) blank membrane surface, pure PVCL microgel-coated surface, PMPC 10000, and PMPC 30000 incorporated zwitterionic microgel-coated surfaces (scale bar 100 μm), (C) absorbance of the leftover protein solution after the protein assay test on respective membranes, (D) the exact amount of protein adsorbed on different membranes; where MG-3X denotes microgels prepared with 3000 g/mol molecular weight PEG-NH₂ cross-linker

UV-vis signal at 495 nm wavelength,⁴⁷ and the absorbance was compared for quantitative detection of attached proteins on the microgel coated membrane. Figure 6C shows that pure PVCL microgel performed relatively better than that of the blank membrane in terms of repelling of the protein molecules as the absorbance of the leftover protein solution is higher for the former than the latter (inset of Figure 6C). The reason could be attributed to the formation of a thin hydration layer by the H-bonding between PVCL chains and the water molecules (see the scheme in Figure 6A). On the other hand, zwitterionic microgel-coated surfaces show the absorbance of leftover protein solution much higher than the PVCL microgel-coated reference membrane due to the formation of a thicker hydration layer by strong electrostatic interaction between opposite charges of zwitterionic backbone and water molecules (see the scheme in Figure 6A). Actually, the presence of highly hydrophilic longer PMPC polyzwitterionic chains in the microgels increases the enthalpy of the system and thus thermodynamically inhibits the nonspecific adsorption of proteins on the membrane surfaces.⁴⁸ The higher is the molecular weight of the PMPC chains, the higher is the absorbance of the leftover protein

solution close to the pure FITC-BSA (100 mg/L) absorbance due to the higher hydrophilicity of the zwitterionic PMPC polymer chains (see inset of Figure 6C). The exact amount of protein adsorbed on the respective surfaces was calculated using a standard calibration line (see supporting information, Figure S10), and on comparing results, the MG-3X series microgels incorporated with PMPC 30000 zwitterionic segments showed considerably much less protein adsorption on its surface than PMPC 10000 zwitterionic segments which quantitatively supports the fluorescence data (see Figure 6D).

To prove our hypothesis of the effect of the cross-linker molecular weight on the hydrodynamic radius and hydration dynamics of the PMPC-PVCL microgels, two zwitterionic microgels with PMPC 20000 and 40000 (molecular weight 20,000 and 40,000 g/mol, respectively) were synthesized using 6000 and 10,000 g/mol molecular weight of PEG-NH₂ cross-linker and the antifouling properties of those microgels were investigated.

As discussed earlier, the higher the PEG-NH₂ cross-linker molecular weight used in the synthesis of zwitterionic microgels, the more difficult it was for the larger PMPC chains to stretch themselves

outwards and penetrate the highly entangled crosslinked PVCL network. Subsequently, the microgels could not form a stronger hydration layer with the water molecules, resulting in a less efficient

antifouling surface coating to resist the protein adsorption appreciably (see the scheme in Figure 7A). When the absorbance of the leftover protein solution was measured by UV-vis study, intriguingly, a striking

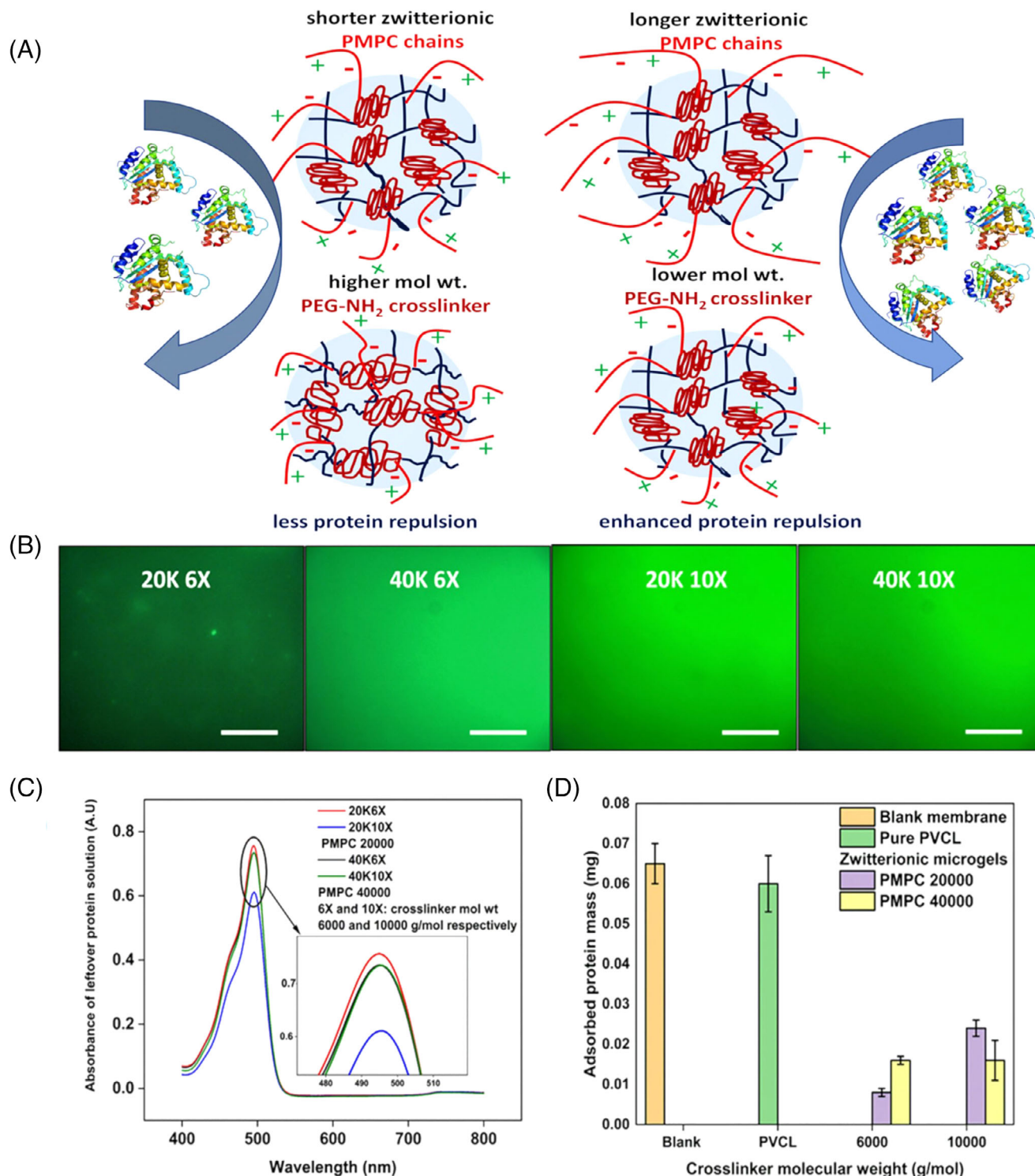


FIGURE 7 (A) Schematic representation of protein repulsion from zwitterionic PMPC-PVCL microgel-coated surface with change in PMPC and crosslinker molecular weight (B) fluorescence microscopic images of different membranes after protein assay test; (from left to right) zwitterionic microgel-coated surfaces with PMPC 20000, PMPC 40000 (6X cross-linker) and PMPC 20000, PMPC 40000 (10X cross-linker) (scale bar 100 μ m), (C) absorbance of the leftover protein solution after the protein assay test on the respective membranes, (D) the exact amount of protein adsorbed on the respective membranes; where 6X and 10X denote 6000 and 10,000 g/mol molecular weight of PEG-NH₂ cross-linker

difference was observed. The MG-20K10X microgel (PMPC 20000 and PEG-NH₂ cross-linker 10,000 g/mol) repelled a lower amount of protein from its surface than the MG-20K6X microgel (PMPC 20000 and PEG-NH₂ cross-linker 6000 g/mol). On the other hand, the PMPC 40000 loaded microgels hardly show any effect on the antifouling behavior with the variation of cross-linker molecular weight (see Figure 7B,C). This can be explained by the relatively larger molecular weight of PMPC 40000, in which the zwitterionic chains have been able to stretch out to their maximum extent by penetrating the comparatively less entangled 6X-crosslinked PVCL network (PEG-NH₂ 6000 g/mol) and this chain movement is independent of a further increase in cross-linker molecular weight. These abovementioned facts can also be justified from the quantitative plot of exact adsorbed protein mass as shown in Figure 7D.

XPS investigations were further carried out to test the protein repellency of the polyzwitterionic microgel coating (MG-40K10X) compared to a pure PVCL microgel coating. As a reference, the BSA adsorption on the clean SiO₂ wafer was also estimated.

C1s, N1s, Si2p, S2p, and P2p core level photoemission signals were recorded and analyzed for all the samples to obtain qualitative and semi-quantitative information about the chemical species present over the sample surface (see Table S7 in SI).

TABLE 3 Evolution of the atomic ratios upon microgel spin-coating

Sample	C/Si	N/Si	S/Si	P/Si	N/C
Blank	0.17	-	0.50	-	-
PVCL	11.79	2.59	-	-	0.23
MG-40K10X	11.87	0.96	-	1.45	0.08

C1s and Si2p core level spectra showed a complex structure and were therefore analyzed by curve fitting. For each C1s spectrum, three components were used, C1-C3, each one referring to a distinct chemical species with typical binding energy (BE): aliphatic carbons (C1, BE = 285.0 eV), C-O or C-N carbons (C2, 286.6 eV), O-C=O and O-C=N carbons (C3, 288.5 eV). Silicon spectra (showed two main components, Si1 (BE ≈ 103.0 eV) related to SiO₂, and Si2, indicating elemental Si (BE ≈ 99 eV). For nitrogen (N1s) core level spectra, the main signal (N1) is located at BE ≈ 400.0 eV typical of amine/amide nitrogens, which cannot be resolved by XPS. The high BE shoulder (N2 BE ≈ 402.0 eV) is related to protonated nitrogens.⁴⁹⁻⁵²

To evaluate the efficiency of microgel deposition on the surfaces, the intensity of the C1s signal was divided by the Si2p total signal (C/Si) as reported in Table 3. The Si2p signal can only come from the surface of the SiO₂ wafer and is therefore supposed to remain constant. The strong increase in the relative intensity of carbon, as well as the appearance of N1s peaks in both the PVCL and MG-40K10X-coated samples prove the efficient immobilization of the microgels on the silica wafer. Additional evidence of efficient microgel deposition is provided by the evolution of the S2p spectra at each step of functionalization. The moderate S2p signal recorded on the blank sensor was probably due to contamination residues present in the analysis chamber. However, after microgel spin-coating, the S2p signal disappears, as expected in the case of the formation of a microgel overlayer in both PVCL and MG-40K10X microgel samples, a hypothesis supported by AFM imaging too (see supporting information, Figure S8).

After immersing the wafer samples in a PBS Buffer dispersion of BSA protein (100 mg/L) at pH 7.4, the C2 peak of the C1s spectra, related to the fraction of the population bound to nitrogen, relatively increases both in the blank and in the PVCL coated wafer (see Figure 8A,B), but decreases in the MG-40K10X zwitterionic microgel

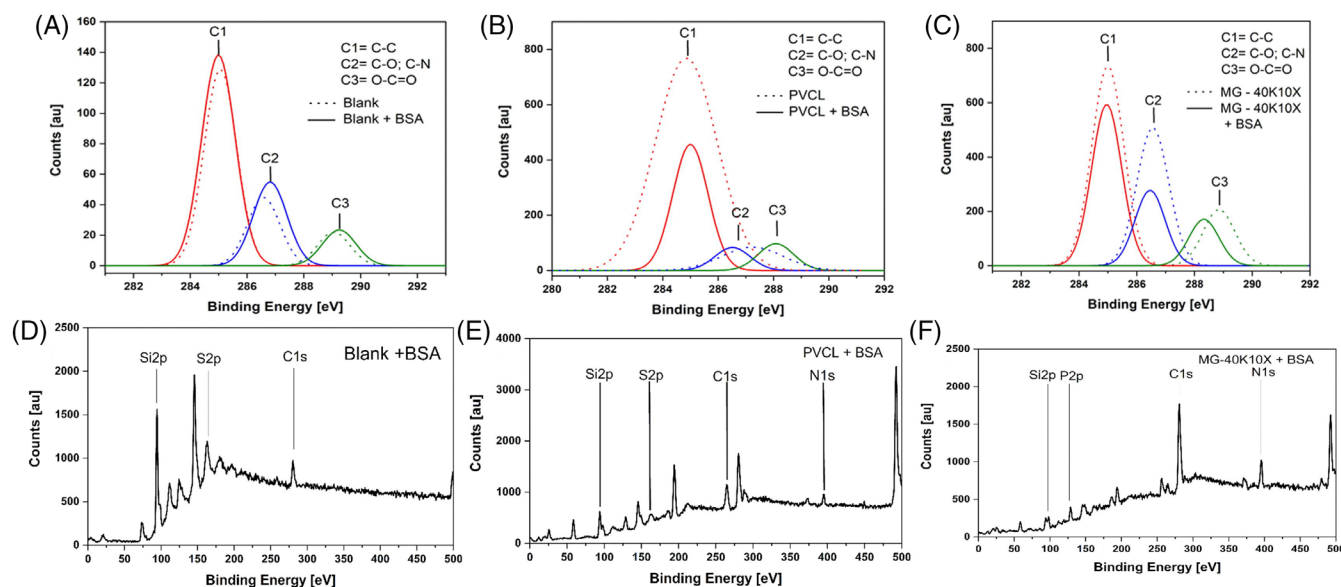


FIGURE 8 Evolution upon BSA treatment of C1s spectra from samples (A) Blank, (B) pure PVCL microgel, and (C) MG-40K10X zwitterionic microgel and overview spectra of BSA-treated samples showing the detected peaks (D) Blank, (E) pure PVCL microgel, and (F) MG-40K10X zwitterionic microgel

TABLE 4 Evolution of the atomic ratios upon immersion in BSA-PBS Buffer dispersion

Sample	C2/C	P/Si	N/C	S/C
Blank	0.23	-	-	2.94
Blank +BSA	0.253	-	-	3.19
PVCL	0.099	-	0.23	-
PVCL+BSA	0.13	-	0.10	0.17
MG-40K10X	0.35	1.45	0.08	-
MG-40K10X + BSA	0.27	0.51	0.12	-

(see Figure 8C). Assuming that the nitrogen detected on the samples coated with PVCL and MG-40K10X is only related to the microgel monolayer, it is possible to use the ratio between the intensity of the N1s signal and the intensity of the C1s signal as a qualitative indicator of the relative abundance of nitrogen that is unique of each coating. As reported in Table 4, upon BSA treatment, a significant decrease in N/C ratio, around 67% was observed, in the surface coated with PVCL, suggesting a remarkable change in the chemical composition of the overlayer that is compatible to the hypothesis of protein adhesion.

As no peaks within the N1s region of the spectrum could be detected, as well as no significant changes in the atomic ratios (including the S/C ratio), on the blank sample was observed, we can conclude that the bare SiO₂ wafer is itself very little prone to protein adhesion (see Figure 8D).

Moreover, traces of S2p, present in the cysteines of BSA, were detected on the same pure PVCL microgel-coated surface, suggesting the occurrence of moderate protein adhesion (see Figure 8E). On the other hand, no peaks in the S2p region could be observed on the spectra collected for the sample MG- 40K10X + BSA, supporting the hypothesis of remarkable protein-repellency (see Figure 8F).

It is thus important to rule out the hypothesis of coating detachment after BSA treatment with the previously coated silica wafer sample with zwitterionic MG-40K10X microgel, to address correctly the absence of protein adhesion on the antifouling microgel surface and not to the exposed bare surface of the native wafer. In this sense, the presence of the poly(phosphobetaine) (PMPC) zwitterionic coating was suggested by the detection of a peak in the P2p region in the particular spectra of 40K10X and 40K10X + BSA, otherwise absent in all other samples, and was ultimately confirmed by AFM imaging (see supporting information, Figure S9). Thus, we can conclude that the microgel coating was itself responsible for the excellent performance as protein repellent.

6 | CONCLUSION

Briefly, we successfully synthesized zwitterionic PMPC-PVCL microgels and integrated the system in the fabrication of antifouling substrates by coating them on poly(ether sulfone) (PES) membranes. The adequate incorporation of PMPC chains in the PVCL-co-PGMA-g-PMPC (PVGP)

graft copolymers underlined the success of this “grafting to” approach for this kind of system. The incorporation of highly hydrophilic polyzwitterionic PMPC groups increased the LCST of the graft copolymer drastically compared to that of the PVG copolymer. Furthermore, the PVGP graft copolymers were converted to PMPC-PVCL microgels, using amphiphilic PEG-NH₂ diamine cross-linker with different molecular weights, adapting a w/o inverse mini emulsion technique. Interestingly, the dual temperature (UCST and LCST) responsiveness of the microgels could be fine-tuned by varying the molecular chain length of both PMPC and PEG-NH₂ diamine cross-linker. The microgels showed appreciable antibio-adhesion properties as well, since they repelled significant amount of incoming protein from their surfaces. The efficacy of the repulsion of protein increased when larger molecular weight of PMPC was used, whereas it decreased upon usage of higher molecular weight of PEG-NH₂ cross-linker. Moreover, the XPS analysis of microgel-coated silica wafers confirmed the superior protein-repellency of the poly(phosphobetaine) (PMPC-PVCL) zwitterionic microgel compared to pure PVCL, as no indicators of protein adhesion could be recorded. This set of results goes on to suggest that these microgel systems have potential to be used in biomedical applications as antifouling components even under challenging conditions.

ACKNOWLEDGMENTS

This paper is dedicated to 70th anniversary of Professor Sarkyt Kudaibergenov. Additionally, the authors thank the Deutsche Forschungsgemeinschaft (DFG), Germany, and the Department of Science and Technology (DST), India for the funding of this project under the DFG-DST joint collaborative research program. The authors would like to thank Dr. Michael Pohl and Mr. Rainer Haas for the GPC data and Mrs. Bea Becker for the FTIR data.

DATA AVAILABILITY STATEMENT

The data that supports the findings of this study are available in the supplementary material of this article.

ORCID

Pabitra Saha  <https://orcid.org/0000-0001-9037-496X>

REFERENCES

1. Lowe S, O'Brien-Simpson NM, Connal LA. Antibiofouling polymer interfaces: poly(ethylene glycol) and other promising candidates. *Polym Chem*. 2015;6:198-212.
2. Knop K, Hoogenboom R, Fischer D, Schubert US. Poly(ethylene glycol) in drug delivery: pros and cons as well as potential alternatives. *Angew Chem Int Ed*. 2010;49:6288-6308.
3. Mrabet B, Nguyen MN, Majbri A, et al. Antifouling poly(2-hydroxyethyl methacrylate) surface coatings with specific bacteria recognition capabilities. *Surf Sci*. 2009;603:2422-2429.
4. Zhao C, Li L, Wang Q, Yu Q, Zheng J. Effect of film thickness on the antifouling performance of poly(hydroxy-functional methacrylates) grafted surfaces. *Langmuir*. 2011;27:4906-4913.
5. Sakharov AM, Mazaletskaia LI, Skibida IP. Catalytic oxidative deformylation of polyethylene glycols with the participation of molecular oxygen. *Kinet Catal*. 2001;42:662-668.

6. Montheard J-P, Chatzopoulos M, Chappard D. 2-Hydroxyethyl methacrylate (HEMA): chemical properties and applications in biomedical. *J Macromol Sci C*. 1992;32:1-34. <https://doi.org/10.1080/15321799208018377>.
7. Sin MC, Chen SH, Chang Y. Hemocompatibility of zwitterionic interfaces and membranes. *Polym J*. 2014;46:436-443.
8. Laschewsky A. Structures and synthesis of zwitterionic polymers. *Polymers (Basel)*. 2014;6:1544-1601.
9. Georgiev GS, Kamenska EB, Vassileva ED, et al. Self-assembly, antipolyelectrolyte effect, nonbiofouling properties of polyzwitterions. *Biomacromolecules*. 2006;7:1329-1334.
10. Iwasaki Y, Ishihara K. Phosphorylcholine-containing polymers for biomedical applications. *Anal Bioanal Chem*. 2005;381:534-546.
11. Ma IY, Lobb EJ, Billingham NC, et al. Synthesis of biocompatible polymers. 1. Homopolymerization of 2-methacryloyloxyethyl phosphorylcholine via ATRP in protic solvents: an optimization study. *Macromolecules*. 2002;35:9306-9314. <https://doi.org/10.1021/ma0210325>.
12. Yusa S, Fukuda K, Yamamoto T, Ishihara K, Morishima Y. Synthesis of well-defined amphiphilic block copolymers having phospholipid polymer sequences as a novel biocompatible polymer micelle reagent. *Biomacromolecules*. 2005;6:663-670.
13. Bhuchar N, Deng Z, Ishihara K, Narain R. Detailed study of the reversible addition-fragmentation chain transfer polymerization and copolymerization of 2-methacryloyloxyethyl phosphorylcholine. *Polym Chem*. 2011;2:632-639.
14. Goda T, Ishihara K. Soft contact lens biomaterials from bioinspired phospholipid polymers. *Expert Rev Med Devices*. 2006;3:167-174.
15. Ishihara K. Highly lubricated polymer interfaces for advanced artificial hip joints through biomimetic design. *Polym J*. 2015;47:585-597.
16. Ladd J, Zhang Z, Chen S, Hower C, Jiang S. Zwitterionic polymers exhibiting high resistance to nonspecific protein adsorption from human serum and plasma. *Biomacromolecules*. 2008;9:1357-1361.
17. Fukazawa K, Nakao A, Maeda M, Ishihara K. Photoreactive initiator for surface-initiated ATRP on versatile polymeric substrates. *ACS Appl Mater Interfaces*. 2016;8:24994-24998.
18. Kuzmyn AR, Nguyen AT, Teunissen LW, Zuilhof H, Baggerman J. Antifouling polymer brushes via oxygen-tolerant surface-initiated PET-RAFT. *Langmuir*. 2020;36:4439-4446. <https://doi.org/10.1021/acs.langmuir.9b03536>.
19. Niskanen J, Tenhu H. How to manipulate the upper critical solution temperature (UCST)? *Polym Chem*. 2017;8:220-232.
20. Niu A, Liaw DJ, Sang HC, Wu C. Light-scattering study of a zwitterionic polycarboxybetaine in aqueous solution. *Macromolecules*. 2000;33:3492-3494.
21. Kikuchi M, Terayama Y, Ishikawa T, et al. Chain dimension of polyampholytes in solution and immobilized brush states. *Polym J*. 2012;44:121-130.
22. Thorne JB, Vine GJ, Snowden MJ. Microgel applications and commercial considerations. *Colloid Polym Sci*. 2011;289:625-646.
23. Wang Y, Guo L, Dong S, Cui J, Hao J. Microgels in biomaterials and nanomedicines. *Adv Colloid Interf Sci*. 2019;266:1-20.
24. Morris GE, Vincent B, Snowden MJ. Adsorption of lead ions onto N-isopropylacrylamide and acrylic acid copolymer microgels. *J Colloid Interface Sci*. 1997;190:198-205.
25. Wang L, Zhang G, Ge JJ, Li G, Zhang J, Ding B. Preparation of microgel nanospheres and their application in EOR. Paper presented at: International Oil and Gas Conference and Exhibition in China, June 8-10, Beijing, China; SPE 130357; 2010.
26. Luo Q, Liu P, Guan Y, Zhang Y. Thermally induced phase transition of glucose-sensitive core-shell microgels. *ACS Appl Mater Interfaces*. 2010;2:760-767.
27. Narayanan R, El-Sayed MA. Effect of catalysis on the stability of metallic nanoparticles: Suzuki reaction catalyzed by PVP-palladium nanoparticles. *J Am Chem Soc*. 2003;125:8340-8347.
28. Meeussen F, Nies E, Berghmans H, Verbrugghe S, Goethals E, du Prez F. Phase behavior of poly(N-vinyl caprolactam) in water. *Polymer (Guildf)*. 2000;41:8597-8602.
29. Tian Y, Lei M, Yan L, An F. Diselenide-crosslinked zwitterionic nanogels with dual redox-labile properties for controlled drug release. *Polym Chem*. 2020;11:2360-2369.
30. Das M, Sanson N, Kumacheva E. Zwitterionic poly(betaine-N-isopropylacrylamide) microgels: properties and applications. *Chem Mater*. 2008;20:7157-7163.
31. Cheng G, Mi L, Cao Z, et al. Functionalizable and ultrastable zwitterionic nanogels. *Langmuir*. 2010;26:6883-6886.
32. Schmid AJ, Schroeder R, Eckert T, Radulescu A, Pich A, Richtering W. Synthesis and solution behavior of stimuli-sensitive zwitterionic microgels. *Colloid Polym Sci*. 2015;293:3305-3318.
33. Schroeder R, Richtering W, Potemkin I, Pich A. Stimuli-responsive zwitterionic microgels with covalent and ionic cross-links. *Macromolecules*. 2018;51:6707-6716.
34. Saha P, Kather M, Banerjee SL, Singha NK, Pich A. Aqueous solution behavior of thermoresponsive polyzwitterionic microgels based on poly(N-vinylcaprolactam) synthesized via RAFT precipitation polymerization. *Eur Polym J*. 2019;118:195-204.
35. Saha P, Santi M, Frenken M, et al. Dual-temperature-responsive microgels from a zwitterionic functional graft copolymer with superior protein repelling property. *ACS Macro Lett*. 2020;9:895-901. <https://doi.org/10.1021/acsmacrolett.0c00304>.
36. De S, Khan A. Efficient synthesis of multifunctional polymers via thiol-epoxy 'click' chemistry. *Chem Commun*. 2012;48:3130-3132.
37. Peng H, RübSam K, Hu C, Jakob F, Schwaneberg U, Pich A. Stimuli-responsive poly(N-Vinyl lactams) with glycidyl side groups: synthesis, characterization, and conjugation with enzymes. *Biomacromolecules*. 2019;20:992-1006.
38. Nishi H, Kobatake S. Reduction reaction to thiol group of dithiobenzoate end group in polystyrene polymerized by reversible addition-fragmentation chain transfer. *Chem Lett*. 2008;37:630-631.
39. Beija M, Marty JD, Destarac M. Thermoresponsive poly(N-vinyl caprolactam)-coated gold nanoparticles: sharp reversible response and easy tunability. *Chem Commun*. 2011;47:2826-2828.
40. Jiang X, Chen Q, Lin S, Shen J. Surface modification of silk fibroin films with zwitterionic phosphobetaine to improve the hemocompatibility. *J Wuhan Univ Technol Mater Sci Ed*. 2010;25:969-974.
41. Jesson CP, Pearce CM, Simon H, et al. H₂O₂ enables convenient removal of RAFT end-groups from block copolymer nano-objects prepared via polymerization-induced self-assembly in water. *Macromolecules*. 2017;50:182-191.
42. Ishihara K, Mu M, Konno T, Inoue Y, Fukazawa K. The unique hydration state of poly(2-methacryloyloxyethyl phosphorylcholine). *J Biomater Sci Polym Ed*. 2017;28:884-899.
43. Saha P, Santi M, Emondts M, et al. Stimuli-responsive zwitterionic core-shell microgels for antifouling surface coatings. *ACS Appl Mater Interfaces*. 2020;12:58223-58238.
44. Lu L, Wang Z, Cao Y. Salt effect on the phase transition behavior of thermo-sensitive polyamide. *J Wuhan Univ Technol, Mater Sci Ed*. 2012;285:285-289.
45. Suwa K, Yamamoto K, Akashi M. Effects of salt on the temperature and pressure responsive properties of poly(N-vinylisobutyramide) aqueous solutions. *Colloid Polym Sci*. 1998;276:529-533.
46. Lalani R, Liu L. Electrospun zwitterionic poly(sulfobetaine methacrylate) for nonadherent, superabsorbent, and antimicrobial wound dressing applications. *Biomacromolecules*. 2013;13:1853-1863.
47. Park S, Lee HJ, Koh WG. Multiplex immunoassay platforms based on shape-coded poly(ethylene glycol) hydrogel microparticles incorporating acrylic acid. *Sensors (Switzerland)*. 2012;12:8426-8436.
48. Liu N, Xu Z, Morrin A, Luo X. Low fouling strategies for electrochemical biosensors targeting disease biomarkers. *Anal Methods*. 2019;11:702-711.

49. Franchi S, Secchi V, Santi M, et al. Biofunctionalization of TiO₂ surfaces with self-assembling oligopeptides in different pH and ionic strength conditions: charge effects and molecular organization. *Mater Sci Eng C*. 2018;90:651-656.
50. Korin E, Froumin N, Cohen S. Surface analysis of nanocomplexes by X-ray photoelectron spectroscopy (XPS). *ACS Biomater Sci Eng*. 2017; 3:882-889.
51. Chen S, Tanaka H. Surface analysis of paper containing polymer additives by X-ray photoelectron spectroscopy I: application to paper containing dry strength additives. *J Wood Sci*. 1998;44:303-309.
52. Greczynski G, Hultmann L. X-ray photoelectron spectroscopy: towards reliable binding energy referencing. *Prog Mater Sci*. 2020; 107:100591-100636.

SUPPORTING INFORMATION

Additional supporting information may be found online in the Supporting Information section at the end of this article.

How to cite this article: Saha P, Palanisamy AR, Santi M, et al. Thermoresponsive zwitterionic poly(phosphobetaine) microgels: Effect of macro-RAFT chain length and cross-linker molecular weight on their antifouling properties. *Polym Adv Technol*. 2021;32:2710-2726. <https://doi.org/10.1002/pat.5214>